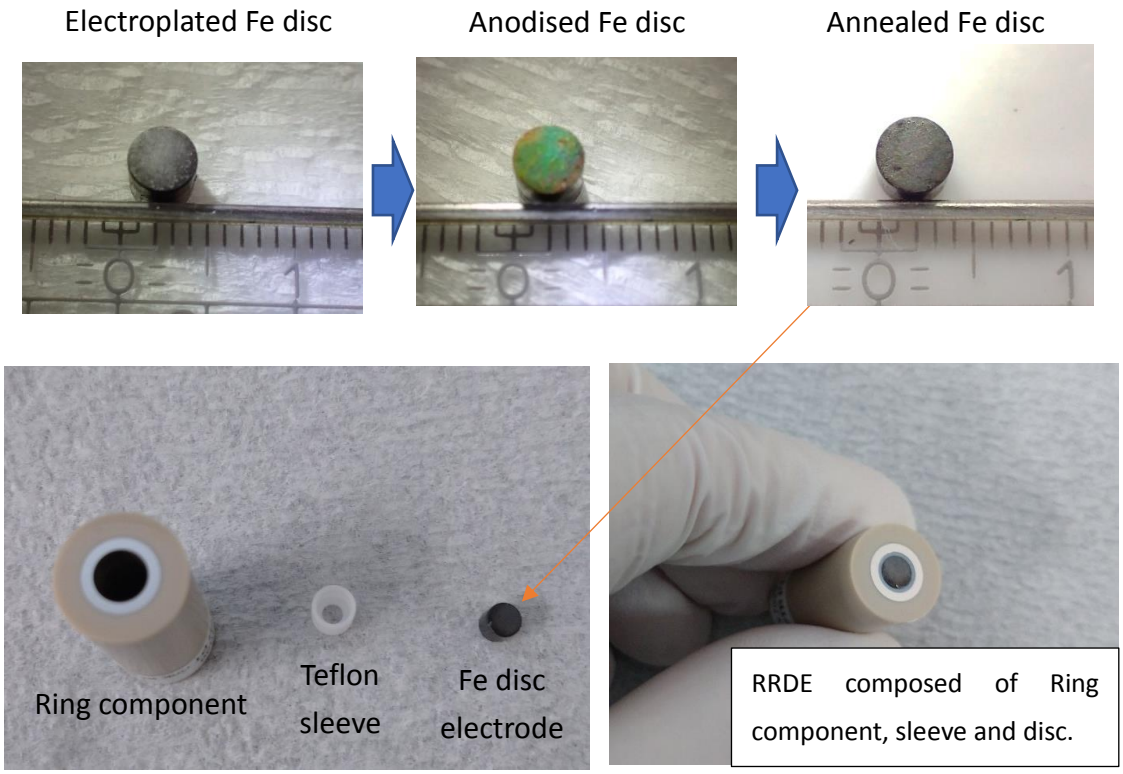

Fig. S1 Photos of Fe discs and components of RRDE. Fe disc in the Teflon sleeve were inserted into the Ring component.

Table S1 Bath composition for electroplating of Fe–Mn alloy films.

Bath Composition	mol dm^{-3}
$FeCl_2 \cdot 4H_2O$	0.05
$MnCl_2 \cdot 4H_2O$	0.5
NH_4Cl	1.0
Trisodium Citrate$\cdot 2H_2O$	0.1

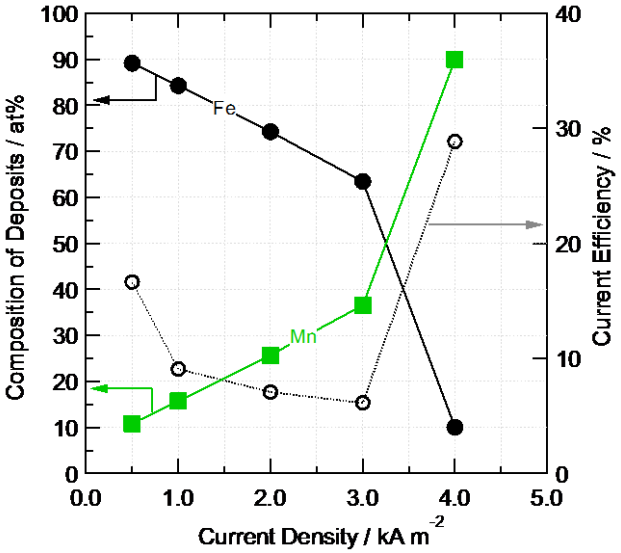

Fig. S2 Effect of current density during electroplating on composition of Fe–Mn deposits and current efficiency.

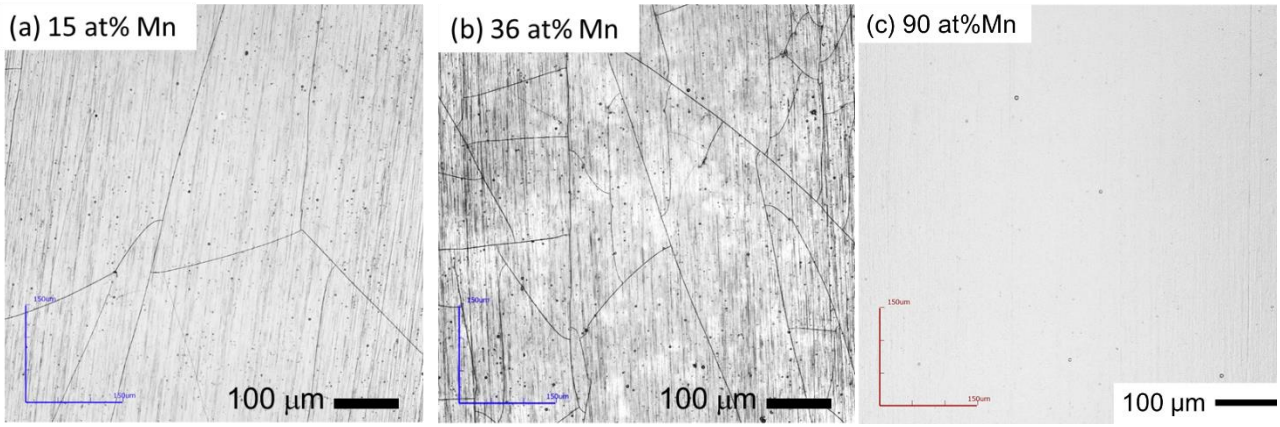

Fig. S3 Laser microscope images of Fe–Mn films with Mn contents of (a) 15 at%, (b) 36 at%, and (c) 90 at%.

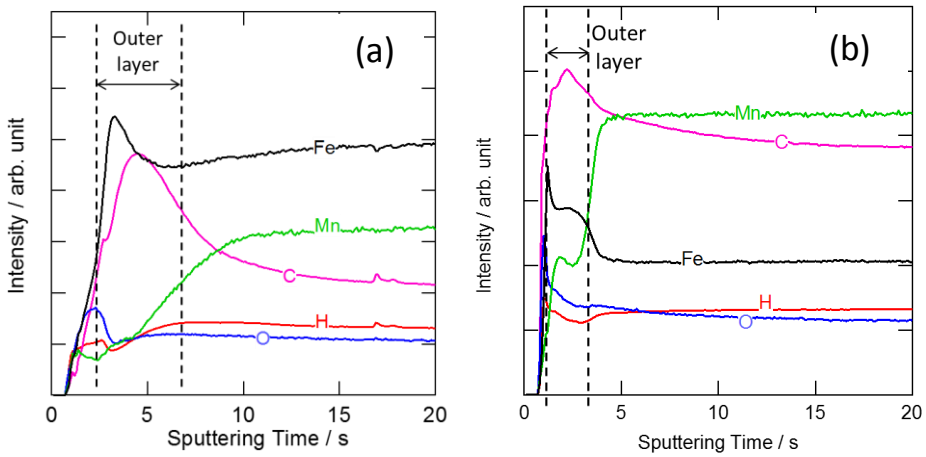

Fig. S4 Elemental GD-OES depth profiles of Fe–Mn film surfaces before anodising: (a) Fe–15 at% Mn, (b) Fe–36 at% Mn.

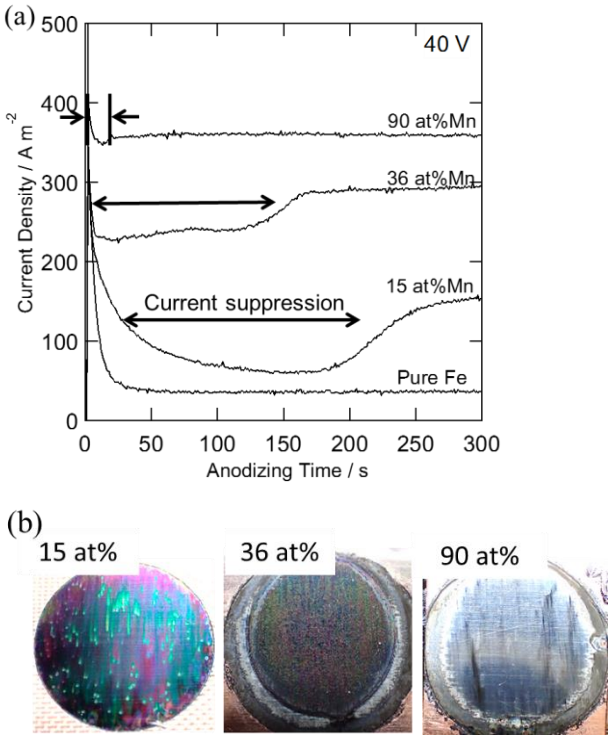

Fig. S5 (a) Current density–time curves recorded during anodising and (b) photographs of Fe–Mn specimens after anodising.

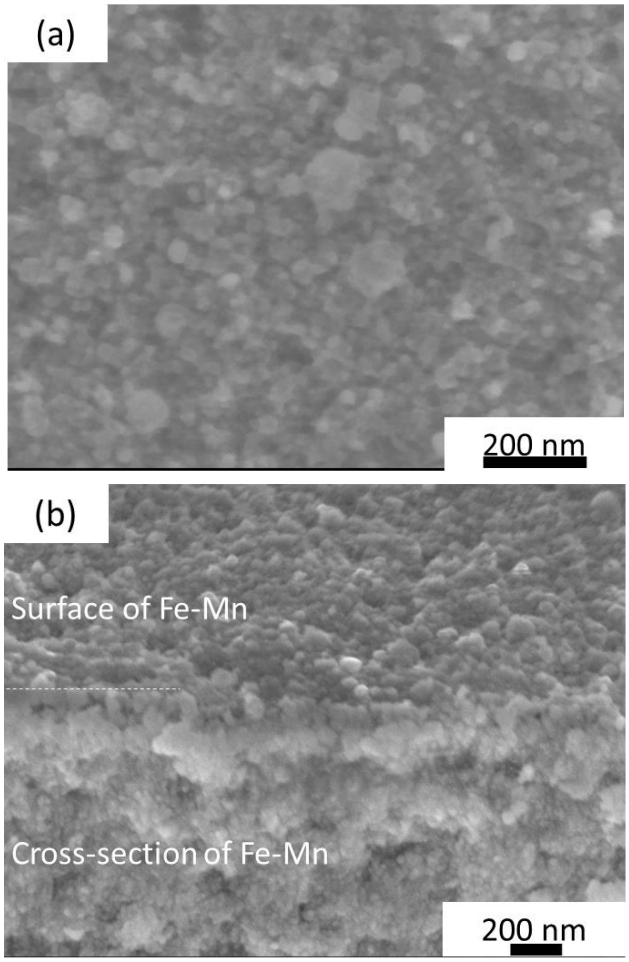

Fig. S6 (a) Surface and (b) fractured cross-sectional scanning electron images of Fe–90 at% Mn electrodeposited film.

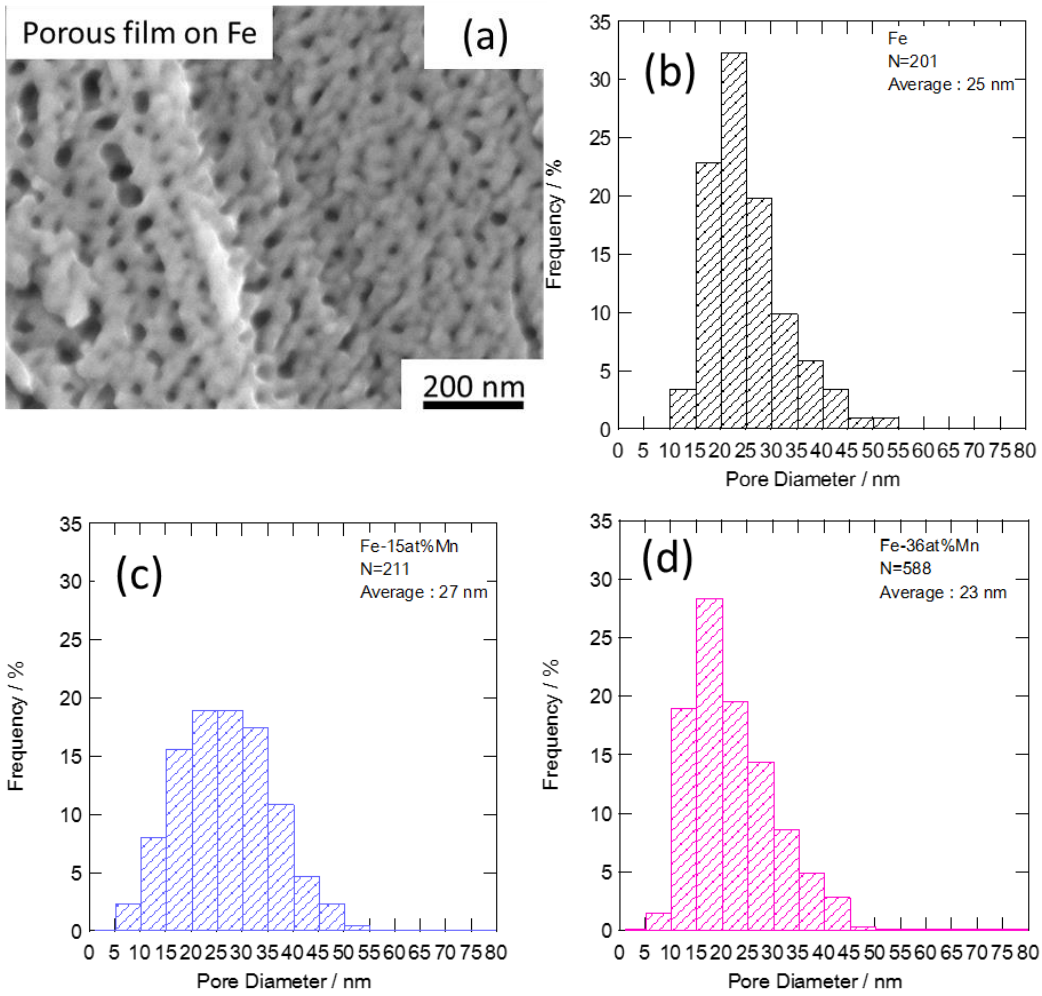

Fig. S7 (a) Electron microscope image of the surface of porous oxide on Fe, (b)-(d) Pore diameter distribution on Fe and Fe-Mn.

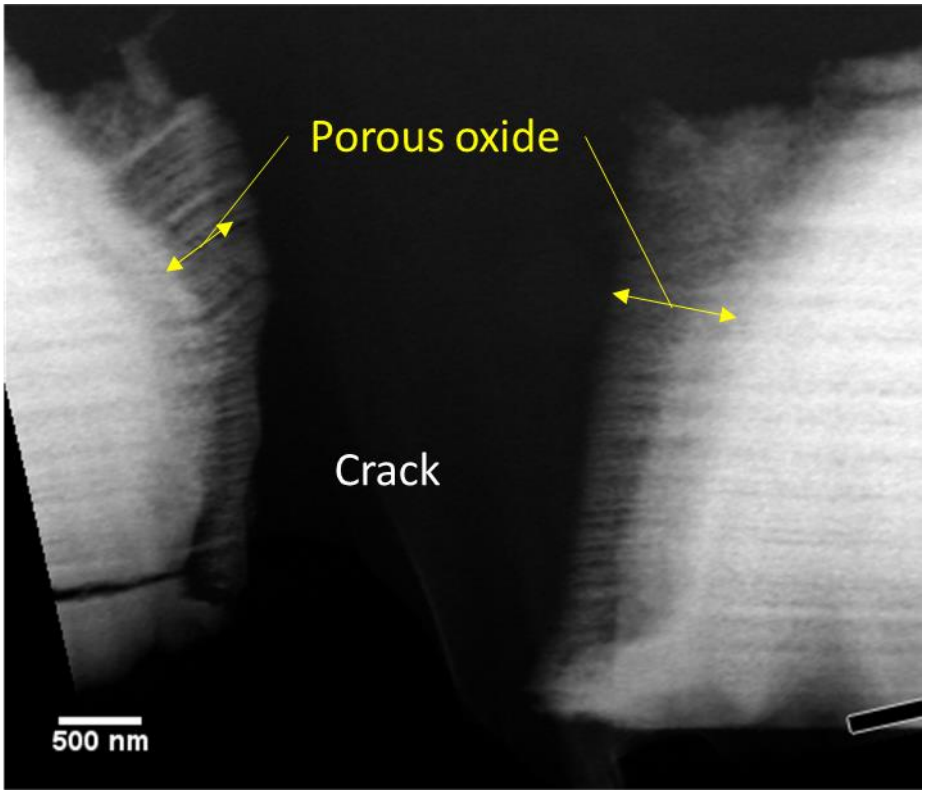

Fig. S8 Cross-sectional dark field TEM image of porous oxide on Fe-36 at% Mn deposited film.

Table S2 Electron transfer number, *n* and kinetic current, I_k estimated from RRDE and K-L analysis at 0.05 V for ORR.

Sample	*n* (estimated from RRDE)	*n* (estimated from K-L)	I_k / mA
Fe	3.78	3.38	4.90
Fe-15at%Mn	3.96	3.87	43.2
Fe-36at%Mn	3.93	4.47	3.85

Table S3 Comparison of the electrocatalyst based on manganese ferrite from the literature in 0.1 mol dm^{-3} KOH for ORR.

No.	Sample	E_{onset}[a] / V vs. RHE	$E_{1/2}$[b] / V vs. RHE	Reference
1	$MnFe_2O_4$ nanoparticles mixed with C	0.88	0.80	S1
2	$MnFe_2O_4$ mixed with XC-72	0.88	0.76	S2
3	Mn-Fe oxide nanopetal on carbonpaper	0.95		S3
4	Al-substituted $MnFe_2O_4$ /rGO	0.92		S4
5	Ag-$MnFe_2O_4$/N, S-codoped graphene	0.908	0.824	S5
6	$MnFe_2O_4$ colloidal nanocrystal assemblies		0.586	S6
7	$Mn_{0.5}Fe_{2.5}O_4$ NP/MC film (Fe-15 at% Mn)	0.88	0.56	This work
8	$MnFe_2O_4$ NP/MC film (Fe-36 at% Mn)	0.88	0.51	This work

[a] Onset potential. [b] half-wave potential.

Table S4 Comparison of the electrocatalyst based on manganese ferrite from the literature in 0.1 mol dm^{-3} KOH for OER.

No.	Sample	E_5[a] / V vs. RHE	E_{10}[b] / V vs. RHE	Tafel slope / mV dec^{-1}	Reference
1	$MnFe_2O_4$ mixed with XC-72		1.82		S2
2	Mn-Fe oxide nanopetal on carbonpaper		1.96	80	S3
3	$MnFe_2O_4$ Nanoparticle	1.87		249.16	S7
4	$MnFe_2O_4$ Nanofiber	1.75		113.62	S7
5	Ag- $MnFe_2O_4$/N, S-codoped graphene		1.75		S5
6	$Mn_{0.5}Fe_{2.5}O_4$ NP/MC film (Fe-15 at% Mn)	1.75	1.79	129	This work
7	$MnFe_2O_4$ NP/MC film (Fe-36 at% Mn)	1.72	1.74	88	This work

[a] Potential at 5 mA cm^{-2}. [b] Potential at 10 mA cm^{-2}.

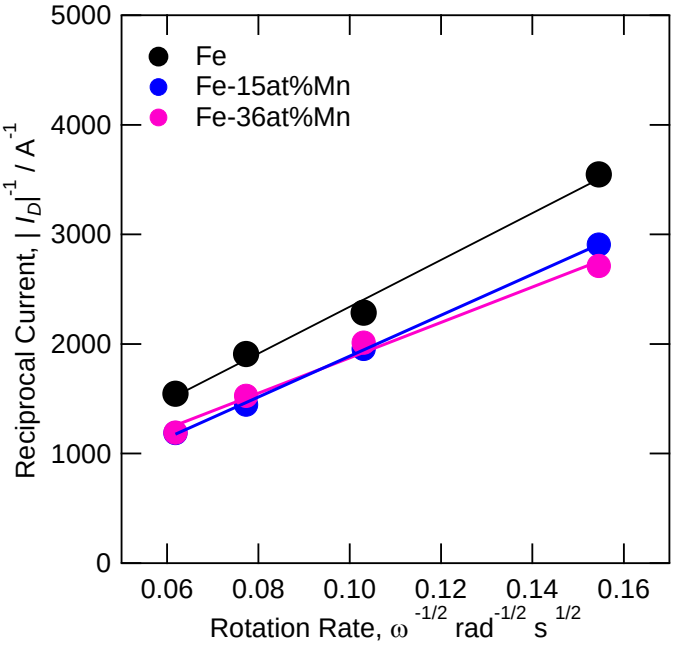

Fig. S9 Koutecky–Levich plots of the porous oxides from the values of measured current at 0.05 V vs. RHE.

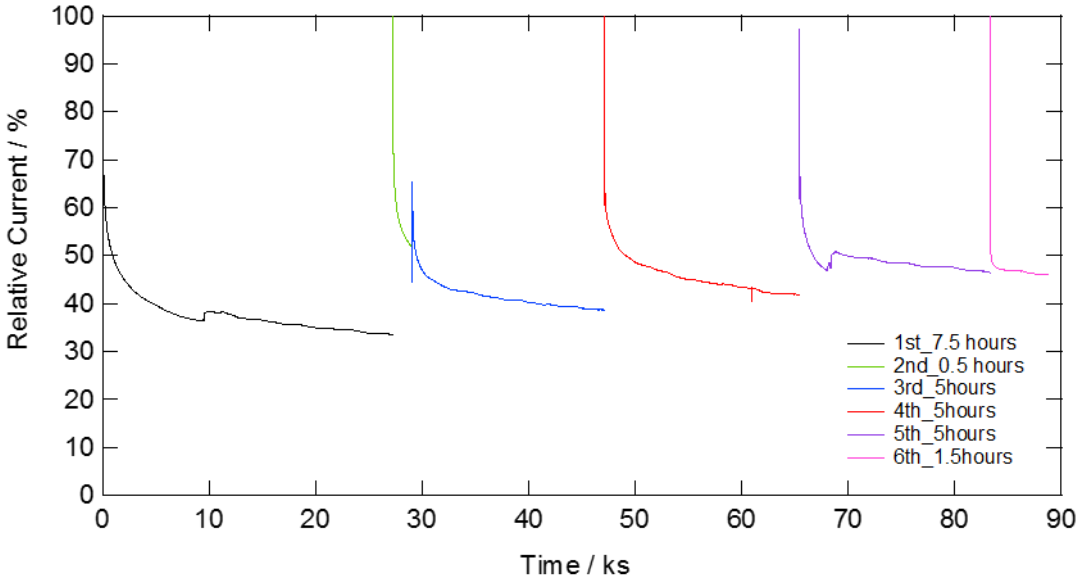

Fig. S10 Relative current of the porous oxide on Fe-15 at% Mn during ORR durability test at a potential of 0.6 V vs. RHE. The durability test was carried out several times for a total of 24 hours.

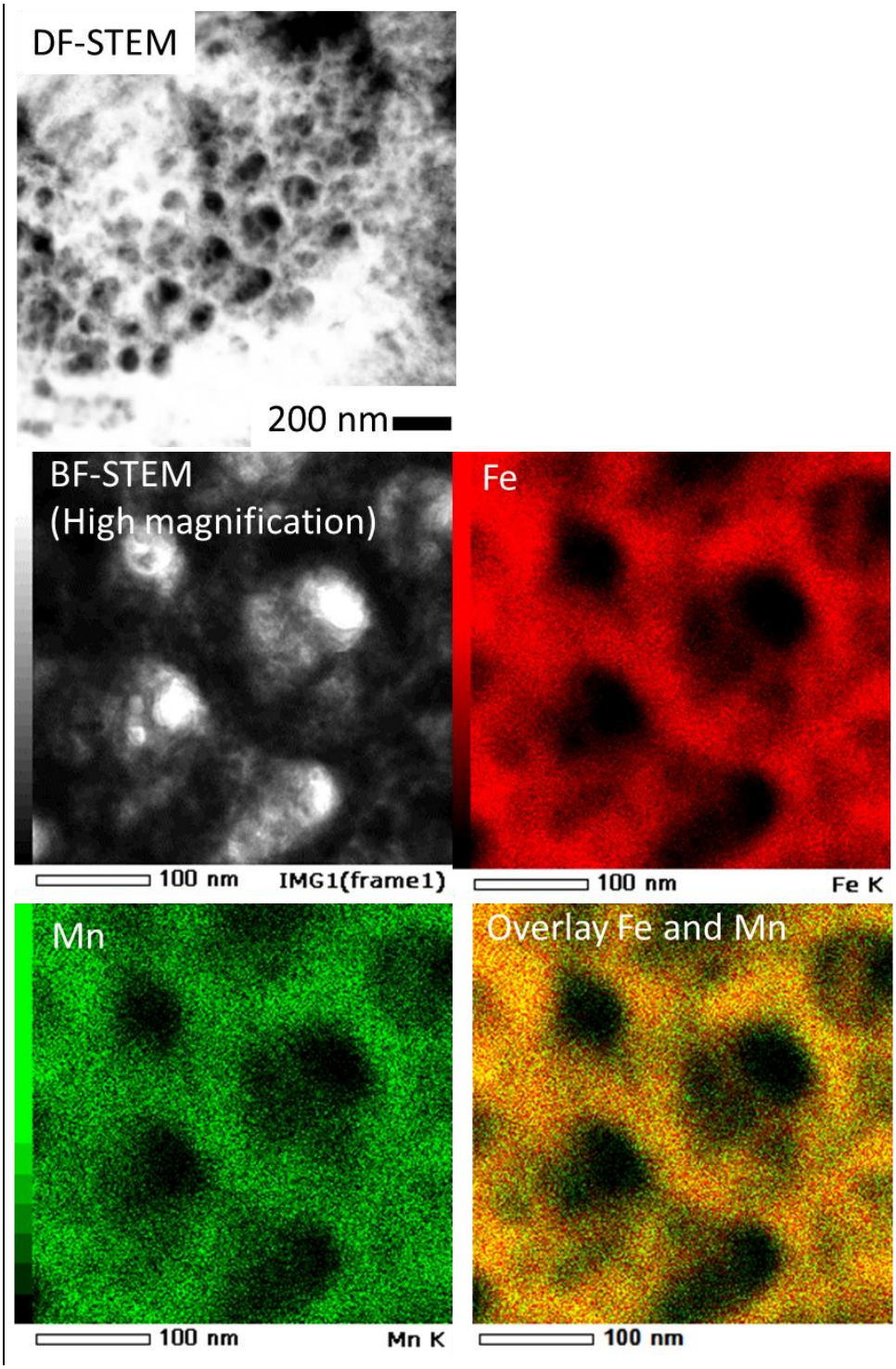

Fig. S11 Dark-field STEM image, Bright-field STEM image and EDX maps on the fragment of porous oxide on Fe-15 at% Mn after ORR durability test for total of 24 h. The oxide fragment was obtained by scratching the electrode.

Table S5 Composition of the porous oxide on Fe-15 at % Mn after ORR durability test for total of 24 h

Element	O	K	Mn	Fe
Composition / at%	57.6	3.3	3.5	35.5

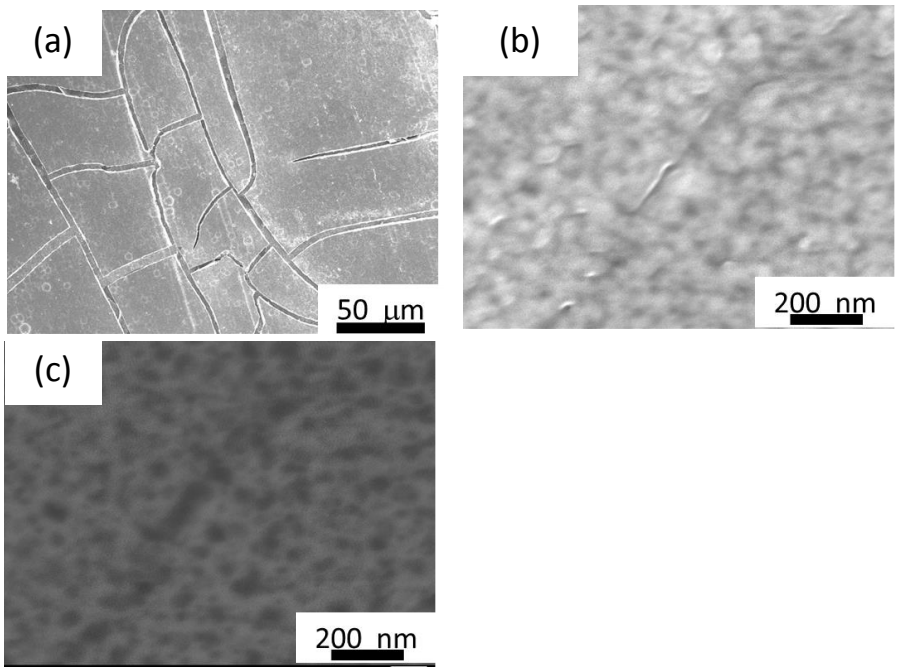

Fig. S12 Electron microscope images of the porous oxide on Fe-15 at% Mn after ORR durability test for a total of 24 h; (a) and (b) the surface images by secondary electron (c) Electron microscope images by back-scattered electrons.

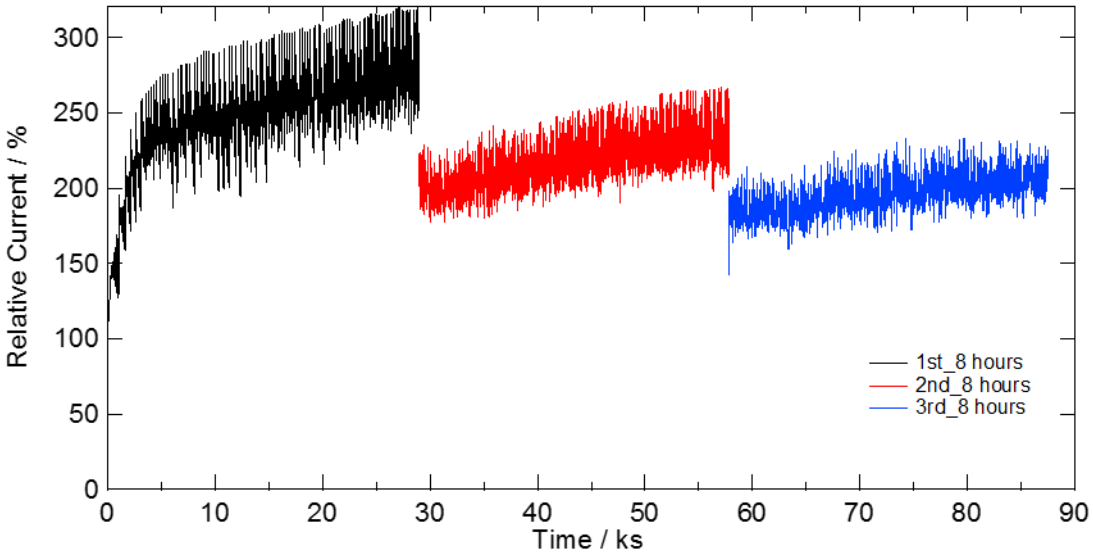

Fig. S13 Relative current of the porous oxide on Fe-15 at% Mn during OER durability test at a potential of 1.8 V vs. RHE. The durability test was carried out 3 times over 8 hour, for a total of 24 hours.

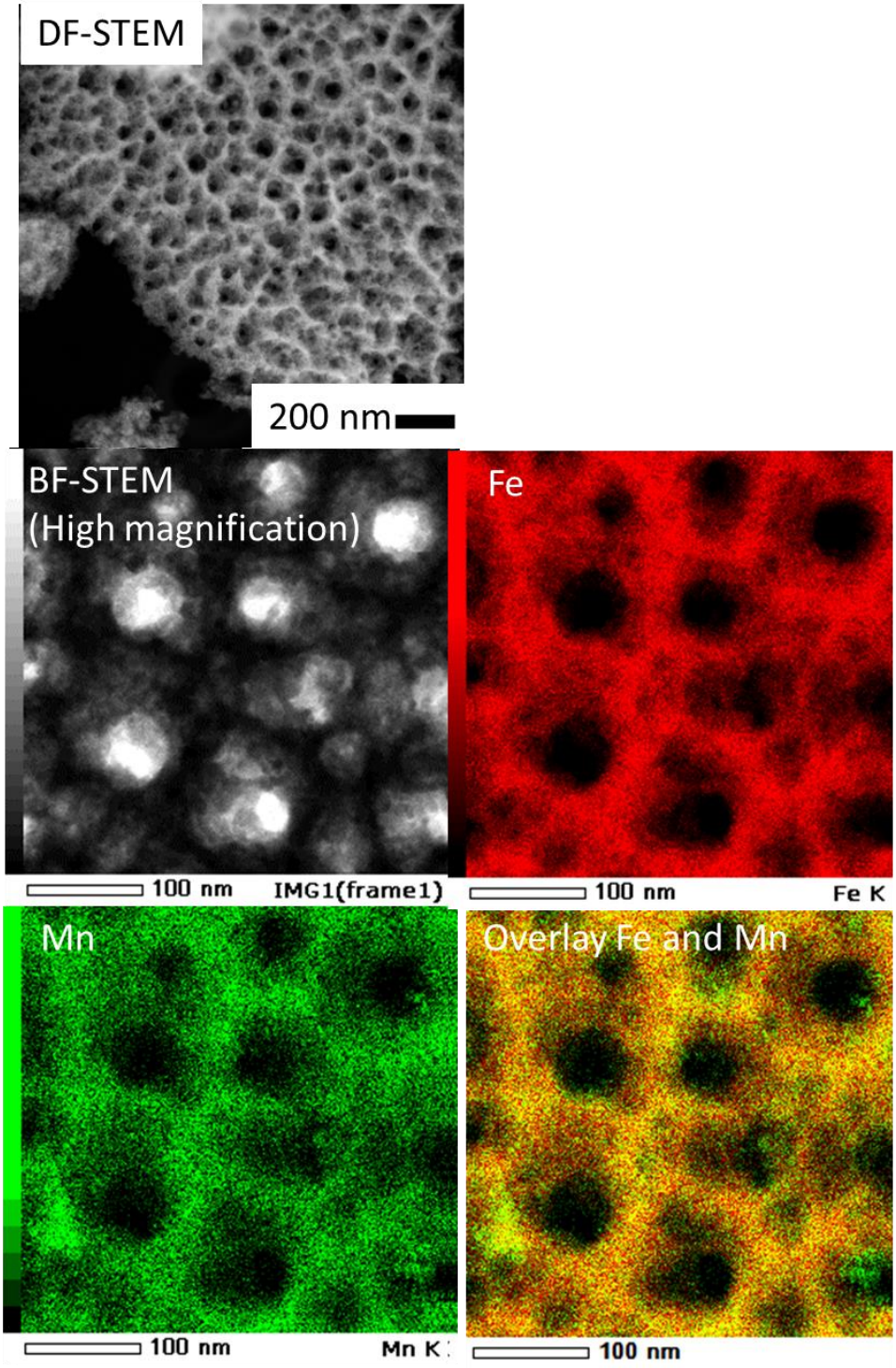

Fig. S14 Dark-field STEM image, Bright-field STEM image and EDX maps on the fragment of porous oxide on Fe-15 at% Mn after OER durability test for a total of 24 h. The oxide fragment was obtained by scratching the electrode.

Table S6 Composition of the porous oxide on Fe-15 at %Mn after OER durability test for total of 24 h

Element	O	K	Mn	Fe
Composition / at%	66.3	0.2	3.5	29.9

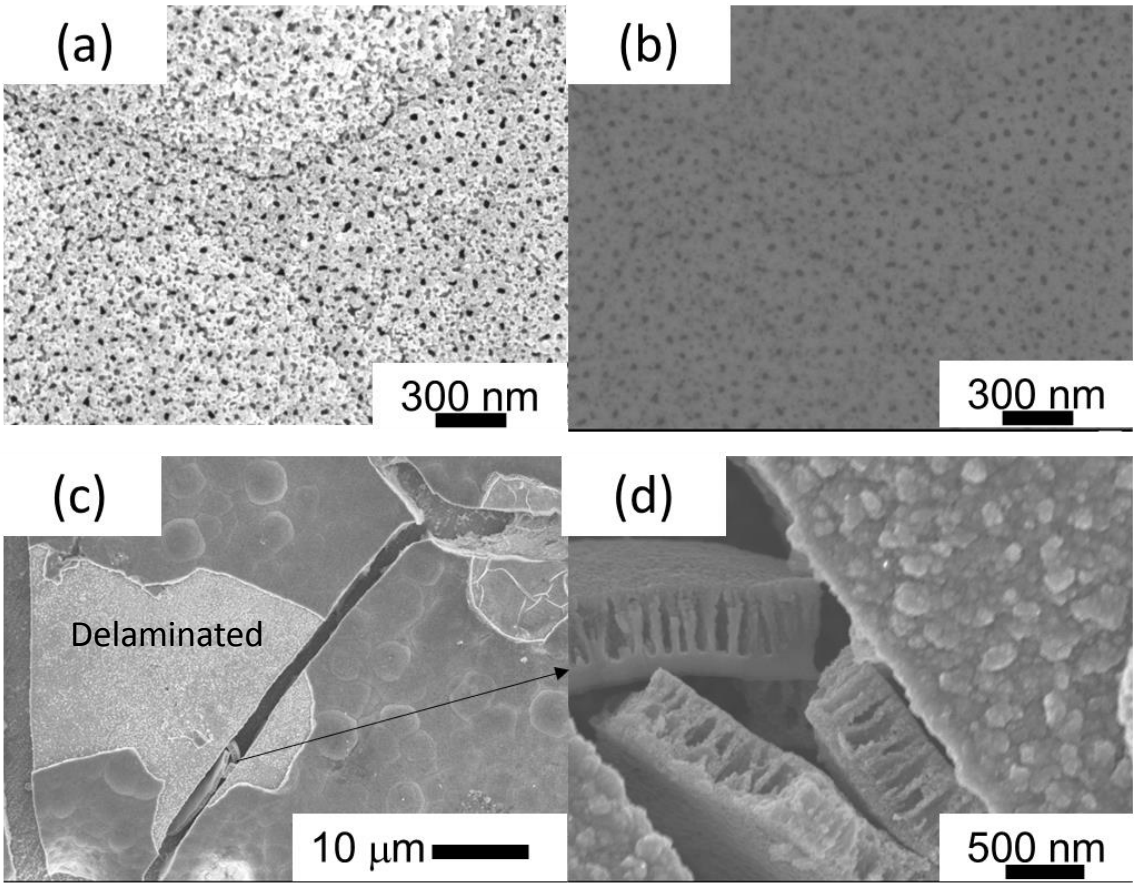

Fig. S15 Electron microscope images of the porous oxide on Fe-15 at% Mn after OER durability test for a total of 24 h; (a), (c) and (d) the surface images by secondary electron (b) Electron microscope images by back-scattered electrons at the same part of (a).

Reference

S1）H. Zhu, S. Zhang, Y.-X. Huang, L. Wu and S. Sun, *Nano Lett.*, 2013, **13**, 2947.

S2）C. Si, Y. Zhang, C. Zhang, H. Gao, W. Ma, L. Lv, Z. Zhang, *Electrochim. Acta*, 2017, **245**, 829.

S3）N.Bhandary, P. P. Ingole and S. Basu, *Int. J. Hydrog. Energy*, 2018, **43**, 3165.

S4）A. Tyagi, Y. K. Penke, P. Sinha, I. Malik, K. K. Kar, J. Ramkumar, H. Yokoi, *Int. J. Hydrog. Energy*, 2021, **46**, 22434.

S5）Y. Chen, Z. Shi, S. Li, J. Feng, B. Pang, L. Yua,W. Zhang, L. Dong, *J. Electroanal. Chem.*, 2020, **860**, 113930.

S6）Zhen Li, Kai Gao, Guangting Han, Rongyue Wang, Hongliang Li, X. S. Zhaoabc and Peizhi Guo, *New J. Chem.*, 2015, **9**, 361

S7）M. Li, Y. Xiong, X. Liu, X. Bo, Y. Zhang, C. Hana and L. Guo, *Nanoscale*, 2015, **7**, 8920.